[6] J. R. Mosig and T. K. Sarkar, "Comparison of quasi-static and exact electromagnetic fields from a horizontal electric dipole above a lossy dielectric backed by an imperfect ground plane," *IEEE Trans. Microwave Theory Tech.*, vol MTT-34, no. 4, pp. 379-387, Apr. 1986.
[7] J. A. Kong, *Theory of Electromagnetic Waves*. New York: Wiley, 1986, ch. 3.
[8] J. A. Stratton, *Electromagnetic Theory*. New York: McGraw-Hill, 1941, pp. 576, Eq (17).
[9] J. Duncan, *The Elements of Complex Analysis*. New York: Wiley, 1968. pp. 214-220.
[10] R. W. Hamming, *Numerical Methods for Scientists and Engineers*. New York: Dover, 1973, pp. 620-622.
[11] M. Marin, S. Barkeshli, and P. H. Pathak, "Efficient analysis of planar microstrip geometries using a closed-form asymptotic representation of the grounded dielectric slab Green's function," *IEEE Trans. Microwave Theory Tech.*, vol 37, no. 4, pp. 669-679, Apr. 1989.
[12] S. Barkeshli, P. H. Pathak, and M Marin, "An asymptotic closed form microstrip surface Green's function for the efficient moment method analysis of mutual coupling in microstrip antennas," *IEEE Trans. Antennas Propagat.*, vol. 38, no. 9, Sept. 1990, pp. 1374-1383.
[13] ——, "Closed form asymptotic representations for the grounded planar single and double layer material slab Green's functions and their applications in the efficient analysis of arbitrary microstrip geometries," presented at the *Int. Conf. on Directions in Electromagnetic Wave Modeling*, New York, Oct. 1990.

Comparison of Measured and Simulated Data in an Annular Phased Array Using an Inhomogeneous Phantom

Dennis M. Sullivan, Dale Buechler, and Frederic A. Gibbs

Abstract—**Computer simulation is being used to plan patient treatments for deep regional hyperthermia in the Sigma 60 applicator of the BSD-2000 Hyperthermia System. The method used is the finite-difference time-domain (FDTD) method. Like all simulation methods, confirmation of the accuracy via measured data is important. Until now, most such measurements in the Sigma 60 were done with homogeneous phantoms. A new phantom using both muscle and fat equivalent material has been constructed, presenting a more challenging simulation problem to the FDTD method. The description of the phantom and the results of comparisons between simulated and measured data are presented.**

I. Introduction

In deep regional hyperthermia cancer therapy, one of the most widely used devices is the Sigma 60 applicator of the BSD-2000 Hyperthermia System (BSD Medical, Salt Lake City, UT). This employs eight dipole antennas positioned around a 60 cm annulus, a configuration known as an annular phased array (APA). The eight dipoles are arranged in four groups of two each, referred to as quadrants. Although the four quadrants are all driven at the same frequency (the frequency range is 60 to 120 MHz), the amplitude and phase on each quadrant can be set independently. This ability to independently set the amplitudes and phases, as well as the selection of the frequency, presents a wide range of input parameters which has motivated the use of computer simulation for treatment planning in the Sigma 60 [1]–[3].

Recently, the implementation of a clinical treatment planning program using the finite-difference time-domain (FDTD) method has been described [4]. The accuracy of this method was tested by comparison of measurements made in a homogeneous phantom. In this paper, further verification will be presented with temperature measurements in an inhomogeneous phantom, which we will refer to as the Utah phantom.

Manuscript received May 31, 1991; revised September 21, 1991. This work was supported by grants CA 29578 and CA 44665 from the National Cancer Institute.

D. M. Sullivan is with the Department of Radiation Oncology, Stanford University School of Medicine, Stanford, CA 94305.

D. Buechler and F. A. Gibbs are with the Division of Radiation Oncology, University of Utah School of Medicine, Salt Lake City, UT 84132.

IEEE Log Number 9105445.

II. Phantom Construction

The Utah phantom used is a CDRH [5] elliptical phantom filled with two materials, one to simulate muscle and one to simulate fat or bone (Fig. 1). The muscle material was constructed from a recipe by Guy [6], with a slight variation: only 75% as much salt was used, giving a material with estimated relative dielectric constant of 60 and conductivity of 0.58 S/m. The fat material was constructed from a recipe by Lagendijk and Nilsson [7], giving a material with a relative dielectric constant of about 8 and a conductivity of about 0.05 S/m.

The phantom was constructed to roughly simulate the lower abdomen and pelvis, although the intent of its design was more that of a buildable inhomogeneous structure than an anatomic simulation. Thirteen catheters were placed in such a way that temperature measurements could be made at enough points to be representative of the SAR pattern within the phantom. The catheters were 16 gauge, large enough to allow easy movement of the temperature probes of the BSD-2000 [8].

III. Experimental Procedure

The energy deposition pattern throughout the phantom was determined by measuring the temperature increase at various points after power was applied for a short period of time in the Sigma 60 applicator. Using three temperature probes at a time, the probes were pushed all the way to the ends of the catheters. The automatic mapping feature of the BSD-2000 was used to move the probes in 1 cm increments, waiting 4 seconds for the temperature measurement to reach equilibrium, and recording it before moving on to the next position. One such reading was made before applying power and another was made after applying 1000 W for 2 min. The temperature difference was then calculated. These temperature differences were compared to the SAR patterns predicted by the FDTD simulation.

To do the FDTD simulation, a model of the phantom was simulated by assigning the corresponding properties of fat or muscle to the 1 cm cells which make up the 3-dimensional model. (This is similar to the way patient models are created for clinical simulations [9].) Approximately 30 000 cells were required for this phantom. The 3-D problem space used to simulate the phantom and the Sigma 60 was $74 \times 74 \times 68 = 372\,368$ cells. This required 10 megawords of core memory and 200 CPU seconds on a Cray YMP supercompter to simulate. Four such runs, corresponding to the four quadrants were necessary to obtain the complex E field at every point in the phantom; the SAR's were determined from these complex E fields. (This is described in detail in [4].)

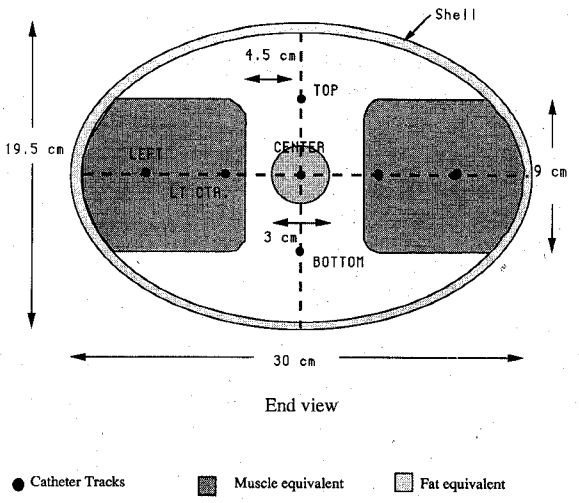

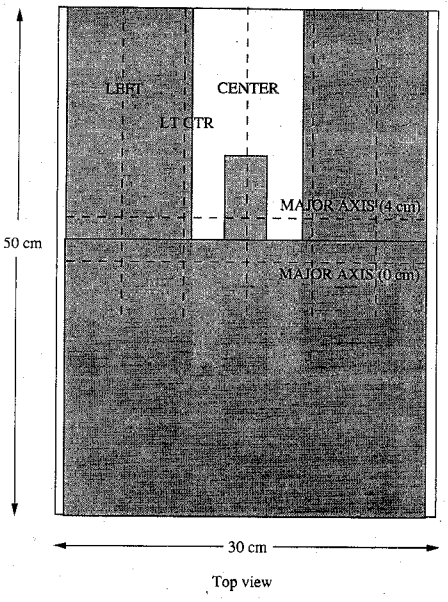

Fig. 1. The Utah phantom. Darker areas represent muscle; lighter areas represent fat. The shell is a material which also simulates fat.

IV. Results

The comparisons between measured and simulated data in the Utah phantom are given in Figs. 2–4. All measurements were done with equal amplitudes and zero phase applied to the four quadrants. The measured temperature increases in each catheter are indicated by blackened squares connected by dashed lines. The SAR's computed by the FDTD program are indicated by dots connected by solid lines. At each frequency, a scaling factor multiplied the calculated SAR by an amount which allowed easy comparison to the temperature rises. (Only one scaling factor is used for all the graphs at that frequency; each graph is not scaled separately.)

Fig. 2 shows the results at 90 MHz. Two key features stand out:

1. The measured data follows the general patterns predicted by the FDTD simulations.
2. The sharp peaks and valleys predicated by the FDTD simulation tend to be "smoothed" by the measured data.

The second observation is not particularly surprising. Remember that the temperature rise is determined by measuring temperature in the catheter before and after applying power in the Sigma 60. There is a time delay when the power is shut off before the temperature can be measured, allowing heat to disperse from a hot point or into a cold point. One would not expect to observe the crisp SAR transitions at the fat/muscle interfaces that the FDTD method can predict, and that may, in fact exist. Another contributing factor may be diffusion of the "fat" and "muscle" material across the fat/muscle interfaces which would tend to smear the actual sharpness of the modelled transitions.

There is only one substantial variation between measured and simulated data: the upper portion of the LEFT catheter. We are unable to account for this discrepancy.

Fig. 3 is a smaller set of compared data for 70 MHz; results are similar. Fig. 4 are the results of comparisons at 110 MHz; these are not as good. Previous comparisons with homogeneous phan-

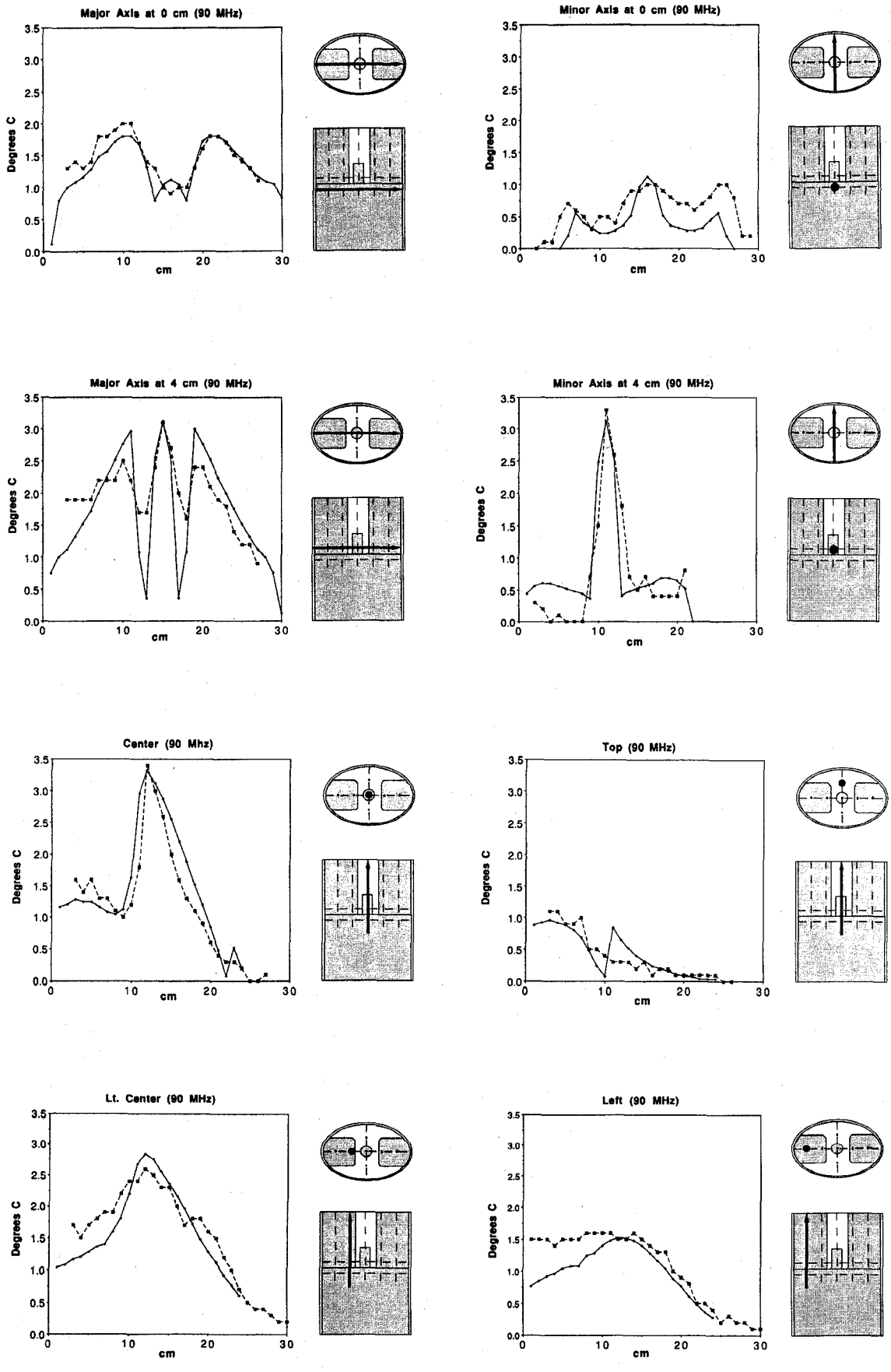

Fig. 2. Comparison of measured and simulated data at 90 MHz. The measured data points are the darkend squares connected by dashed lines; the points calculated by the FDTD method are dots connected by solid lines.

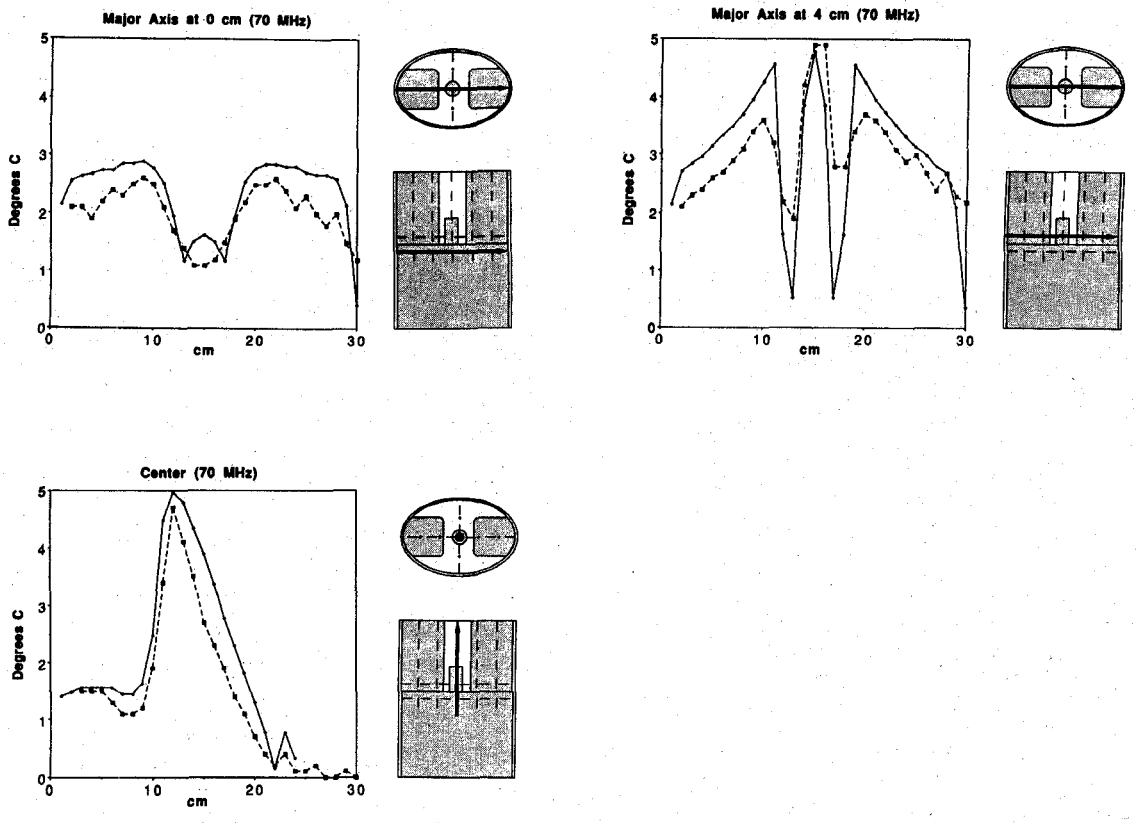

Fig. 3. Comparison of measured and simulated data at 70 MHz. The measured data points are the darkend squares connected by dashed lines; the points calculated by the FDTD method are dots connected by solid lines.

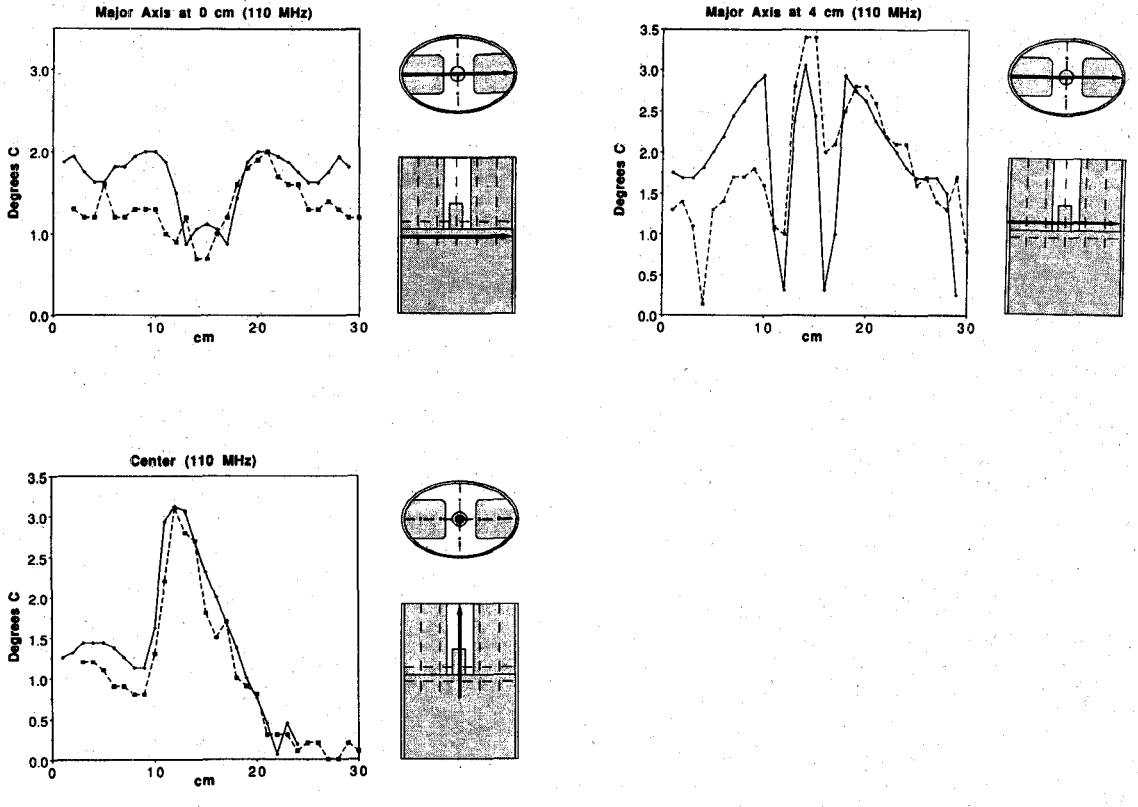

Fig. 4. Comparison of measured and simulated data at 110 MHz. The measured data points are the darkend squares connected by dashed lines; the points calculated by the FDTD method are dots connected by solid lines.

toms also showed less favorable comparison between measured and simulated data at the higher frequencies. It has been speculated that this could be due to higher cross-talk among the quadrants [10] or a change in the current pattern on the dipoles [11] at the high frequencies. Nonetheless, the measured data still follows the general pattern of the FDTD data.

V. Discussion

We have presented comparisons between measured data from an inhomogeneous phantom and those predicted by an FDTD program used in treatment planning for deep regional hyperthermia. These were limited to the case of equal amplitudes and phases at three frequencies. A more extensive range of comparisons for different configurations of amplitude and phase would be desirable, but the number of measurements is hindered by time-consuming logistical problems. The Utah phantom itself requires almost two days to construct and suffers from a short "shelf life" due to the materials used and boundary diffusion. However, this phantom represents a substantial improvement over conventional homogeneous phantoms in testing the ability of simulation methods to account for the inhomogeneities of the human body. In particular, it is hoped that the results presented here will promote confidence in the treatment planning program using the FDTD method.

References

[1] M. F. Iskander, P. F. Turner, J. T. DuBow, and J. Koa, "Two-dimensional technique to calculate the EM power deposition pattern in the human body," *J. Microwave Power*, vol. 17, pp. 175–185, 1982.

[2] V. Sathiaseelan, M. F. Iskander, G. C. Howard, and N. M. Bleehen, "Theoretical analysis and clinical demonstration of the effect of power pattern control using the annular phased-array hyperthermia system," *IEEE Trans Microwave Theory Tech.*, vol. MTT-34, pp. 514–519, 1986.

[3] C. Wang, and O. P. Gandhi, "Numerical simulation of annular phased arrays for anatomical based models using the FDTD method," *IEEE Trans. Microwave Theory Tech.* vol. 37, pp. 118–126, 1989.

[4] D. M. Sullivan, "Mathematical methods for treatment planning in deep regional hyperthermia, *IEEE Trans. Microwave Theory Tech.*, vol. 39, pp. 864–872, May 1991.

[5] S. Allen, G. Kantor, H. Bassen, and P. Ruggera, "CDRH RF phantom for hyperthermia systems evaluation," *Int. J. Hyperthermia*, vol., pp. 17–23, 1988.

[6] A. W. Guy, "Analyses of electromagnetic fields induced in biological tissues by thermographic studies on equivalent phantom models," *IEEE Trans. Microwave Theory Tech.*, vol. MTT-19, pp. 205–214, Feb. 1971.

[7] J. J. W. Lagendijk and P. Nilsson, "Hyperthermia dough: a fat and bone equivalent phantom to test microwave/radio frequency hyperthermia heating systems," *Physics in Medicine and Biology*, vol. 30, pp. 709–712, July 1985.

[8] R. R. Bowman, "A probe for measuring temperature in radio frequency heated material," *IEEE Trans. Microwave Theory Tech.*, vol. MTT-24, pp 43–45, Jan. 1976.

[9] B. J. James and D. M. Sullivan, "Creation of three dimensional patient models for hyperthermia treatment planning," *IEEE Trans. Biomed. Eng.*, vol. 39, no. 3, March 1992.

[10] L. B. Leybovich, R. J. Myerson, B. Emami, and W. L. Straube, "Evaluation of the Sigma-60 applicator for regional heating in terms of scattering parameters," presented at the *9th Annual Meeting of the North American Hyperthermia Group*, Seattle, WA, Mar. 1989.

[11] P. Wust *et al.*, "Einflussfaktoren und stoereffekte bei der steuering von leistungsverteilungen mit dem hyperthermi-ringsystem BSD-2000. II. Messtechnische analyze," *Strahlungtherapie Onkologie*, to be published.

Alternative Field Representations and Integral Equations for Modeling Inhomogeneous Dielectrics

John L. Volakis

***Abstract*—New volume and volume-surface integral equations are presented for modeling inhomogeneous dielectric regions. In particular, it is shown that materials with non-trivial permeability and permittivity can be modeled using a single unknown equivalent current or field component. The presented integral equations result in more efficient numerical implementations and should therefore be useful in a variety of electromagnetic applications.**

I. Introduction

The modeling of inhomogeneous dielectrics via an integral equation approach is traditionally accomplished via the introduction of equivalent volume electric and magnetic currents [1]–[8]. For a dielectric with non-trivial permittivity and permeability this type of modeling implies six scalar unknowns at each volume location. As a result, the implementation of the resulting integral equation is computationally intensive and has excessive storage requirements.

In this paper it is demonstrated that any inhomogeneous dielectric material, regardless of its permittivity and permeability profile, can be modeled by a single electric or magnetic current density. Alternatively, either the electric or magnetic fields within the dielectric can be used as the unknown quantities. It appears though that one must pay a price for resorting to these reduced-unknown and/or kernal-singularity representations. Specifically, because they involve derivatives of the unknown quantities, a higher (at least linear) basis function is required for discretizing the resulting integral equations. However, it is possible to relax this requirement by resorting to a new volume-surface field representation. In this case, the undifferentiated electric or magnetic field within the dielectric is the unknown quantity along with the corresponding tangential electric or magnetic fields on the outer boundary. Provided the dielectric volume is not composed of a single thin layer, this volume-surface integral equation still represents a nearly fifty percent reduction in the number of unknowns relative to traditional implementations.

II. Volume Representations

Let us consider the dielectric/ferrite volume V_d, shown in Fig. 1, having relative constitutive parameters ϵ_r and μ_r which are arbitrary functions of position. Assuming some exterior excitation, $(\boldsymbol{E}^i, \boldsymbol{H}^i)$, the total field can be written as

$$\boldsymbol{E} = \boldsymbol{E}^i + \boldsymbol{E}^s \quad \boldsymbol{H} = \boldsymbol{H}^i + \boldsymbol{H}^s \tag{1}$$

where $(\boldsymbol{E}^s, \boldsymbol{H}^s)$ are the scattered fields caused by the presence of the dielectric. Traditionally [1] the scattered fields are formulated

Manuscript received July 10, 1991; revised October 30, 1991.

The author is with the Radiation Laboratory, Department of Electrical Engineering and Computer Science, University of Michigan, Ann Arbor, MI 48109-2122.

IEEE Log Number 9105442.